L-shell filling of N^{6+} and O^{7+} ions from a clean and LiF-covered Au(111) surface

H. Khemliche,* T. Schlathölter, R. Hoekstra, and R. Morgenstern
KVI Atomic Physics, Rijksuniversiteit Groningen, Zernikelaan 25, NL-9747 AA Groningen, The Netherlands
(Received 23 April 1999)

We report on a high-resolution Auger spectroscopy study of the interaction of N^{6+} and O^{7+} ions with a clean and a LiF-covered Au(111) target. The electron spectra from collisions on Au(111) and LiF-covered Au(111) are distinctly different. The ones resulting from the interaction with Au(111) covered with one monolayer of LiF resemble spectra taken on bulk LiF, which, in contrast to LiF-covered Au(111), is an insulator. On the Au(111) surface and for scattering geometries preventing projectile penetration below the first atomic layer, a more efficient *L*-shell filling for O^{7+} than for N^{6+} ions is observed. Surprisingly enough, for a single monolayer of LiF on Au the total *K* Auger intensity of nitrogen is nearly 30% larger as compared to the clean Au(111) target, while for oxygen no enhancement is found. These findings demonstrate that, for specific projectile-target systems (e.g., N-LiF), an efficient mechanism that fills the projectile *L* shell is active well before the projectiles reach the surface, so that *KLL* electrons are emitted at an early stage of the interaction. [S1050-2947(99)04010-X]

PACS number(s): 34.50.Dy, 34.50.Rk, 34.70.+e, 82.30.Fi

I. INTRODUCTION

The interaction of multiply charged ions with solid surfaces has been the subject of numerous studies in the past few years and the main features of the neutralization are relatively well described qualitatively (for a review, see [1]). However, a detailed and quantitative understanding has not yet been reached. The extreme character of the system under consideration, high electron depletion on one side and large densities of loosely bound electrons on the other side, is certainly the source of many subtle processes not yet revealed. Moreover, the diversity of experimental techniques available makes a synthesis difficult since each one of them only views the interaction through a specific window. Additionally, the use of different projectile-target systems and different experimental conditions prevents a direct comparison between experiments. Thus many aspects remain unresolved, such as the dynamics of the hollow atom/ion in front of the surface, the mechanisms responsible for the early population of inner shells, and the sensitivity of the neutralization to various properties of the target (e.g., electron density and mobility, band structure, band gap for insulators, etc.).

The neutralization of highly charged ions above a metal surface is most often described using the classical over-the barrier (COB) model [2–4]. According to this model, the first phase of the neutralization consists of a competition between capture of conduction electrons into the ion excited orbitals and electron loss through autoionization and resonant ionization. In the latter process, the projectile electron loss into the empty states of the conduction band allows the capture of another electron into a lower projectile level, thus speeding up the population of the lower shells. Due to the short time available for the above-surface interaction, the Auger cascades alone cannot account for the *KLL* Auger emission above the metal surface as observed experimentally by several authors [5–8]. Therefore, resonant ionization followed by capture might have a direct effect on the early population of inner shells [9]. Recent studies on insulators (LiF) seem to indicate that the above-surface *KLL* Auger emission is strongly suppressed [10]. Bulk LiF has a high binding energy (12 eV) of valence electrons and a large band gap (14 eV). On the grounds of the above-mentioned COB model, both quantities could be held responsible for the suppression of the *KLL* Auger emission above the surface. In addition to the disappearance of the usual signature of the above-surface component in the Auger spectra, Limburg *et al.* [10] observed a shift of the low-energy side of the spectra by $\approx$10 eV towards lower energies. A satisfactory understanding of the observed behavior could not be achieved since several properties are changed simultaneously when going from a metal (e.g., Au) to an insulator such as LiF (see Fig. 1).

Ideally, one wishes to change continuously target properties from metals to insulators; this can be achieved at least partly by using thin-film covered targets. The properties of thin LiF films have been investigated [11] and, for very thin films, the binding energy of valence electrons is already

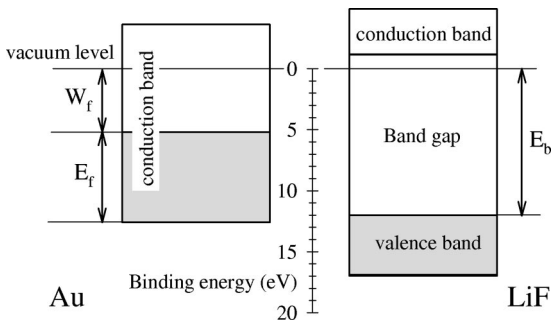

FIG. 1. Schematic representation of the electronic structures of Au and bulk LiF.

*Present address: Laboratoire des Collisions Atomiques et Moléculaires, Bât. 351, Université Paris–Sud, F-91405 Orsay Cedex, France.

close to that of bulk LiF. However, the band gap develops only around five monolayers (ML). Consequently, the use of very thin LiF films is an appropriate method for accessing the role of certain properties of a LiF surface in the neutralization of highly charged ions. In order to gain information on the respective importance of the binding energy and the band gap in the neutralization of multiply charged ions on LiF, and thus to get insight into the above-surface interaction, we have investigated the *KLL* Auger emission from grazing incidence impact of hydrogenlike N^{6+} and O^{7+} ions on a clean and a LiF-covered Au(111) surface. It is known that the neutralization dynamics depends on the target-projectile system. For instance it was observed that for bulk LiF as a target, N^{6+} and O^{7+} ions have different inner-shell filling rates [12]; that was explained by differences in their inner-shell binding energies. Consequently, the controlled surface modification, together with the use of N^{6+} and O^{7+} projectiles, gives us the ability to effectively access details of the interaction. The efficiency of the inner-shell filling can be estimated from the structures in the *KLL* Auger spectrum and their dependence on the observation angle. Together with the measured Doppler shift, it is possible to evaluate the spatial origin of the *KLL* Auger electrons. To strengthen conclusions on the spatial origin of the *KLL* Auger emission, we performed trajectory calculations using the MARLOWE code [13]. After presenting the experimental procedure and trajectory simulations, we will present first measurements of the angular variation of the Auger spectra obtained on a clean Au(111) surface and further use that information for interpreting the results from the LiF-covered Au target.

II. EXPERIMENTAL PROCEDURE

Before each deposition cycle, the Au(111) surface was sputter cleaned with 1 keV Ar^+ and annealed at 400 °C. The surface cleanness was checked by low-energy ion scattering (LEIS) and the surface morphology was asserted from the quality of the intensity structures of scattered He projectiles observed in the crystal azimuthal scan. LiF molecules were evaporated from an electron impact heated crucible filled with a LiF powder. The evaporator was water-cooled so that during operation the base pressure in the main chamber remained in the low 10^{-8} Pa range. The deposition system is equipped with a flux monitor, which assures a reproducible evaporation dose. The film growth was analyzed with LEIS using 1 keV He^{2+} ions [14–16]. The energy spectrum of the scattered ions comprises peaks resulting from elastic scattering of He^{2+} from the surface atoms; the integrated peak intensity is proportional to the atom surface density. At a constant LiF evaporation flux, the variation of relative contributions from scattering off LiF (sum of scattering from Li and F) and Au with deposition time follows at higher coverages a nonlinear behavior (Fig. 2). That could be due to either a multilayer growth or simply to a change in the sticking coefficient during the growth. To overcome the influence of the latter effect, we have deposited a closed LiF layer (no Au component observable in the LEIS spectrum) and then monitored the LiF coverage during sputtering of the film by the probing beam. The LiF sputtering rate by He ions is high enough to permit such a measurement [17]. The subsequent relative LEIS signals from LiF and Au are linear in time

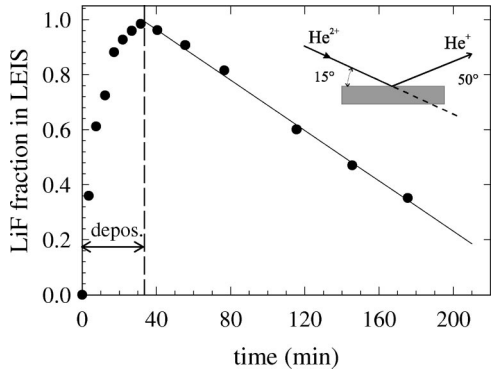

FIG. 2. Evolution of the LiF contribution (sum of scattering from Li and F atoms) to the total amount of scattered He^+ ions. The left-hand side corresponds to the coverage variation during deposition, which was stopped at the time indicated by the dashed line. The right-hand side corresponds to the coverage variation induced by sputtering by the probing He^{2+} beam. The solid line is a linear fit to the data.

(Fig. 2), indicating that the film growth was proceeded by completion of a single monolayer [18]. Thus the deposition system could be calibrated and the time necessary for the deposition of one monolayer LiF determined. The absence of the band gap could be verified by He^+ scattering and measuring the survival probability of incident ions. The latter did not show any substantial increase when going from Au to 1 ML LiF on Au, whereas the existence of a large band gap would lead to an order of magnitude increase in the survival probability of ions through the suppression of Auger neutralization [19].

A drawback of the large sputtering rate of LiF [20] is the difficulty to maintain a steady coverage while a multiply charged ion beam impinges on the film. This limitation is minimized by using low beam intensities and as short as possible scanning times. A whole series of *KLL* Auger spectra is recorded following the deposition of 1 ML LiF. The change in the coverage is monitored in between measurements by measuring the relative contribution of the elastic scattering from LiF in the energy spectra of the reflected ions. As an example, Fig. 3 shows the reflected O^{2+} ion spectra from 6.15 keV O^{7+} incident at $\psi = 10°$. These ions, detected off specular reflection, offer a great surface sensitivity. The top spectrum results from a clean Au(111); then following deposition of one LiF monolayer, the three bottom spectra are recorded. During acquisition, the LiF overlayer is being sputtered by the incident ions. Thus the LiF coverage decreases from bottom to top. We distinguish O^{2+} scattered off Au and F surface atoms; one can notice the large intensity difference between ions reflected from a clean Au (top) and 1 ML LiF on Au (bottom), indicating a higher survival probability of O^{2+} against neutralization by LiF.

III. SCATTERING GEOMETRIES

Before discussing the experimental data it is important to have an idea about scattering geometries and trajectories followed by the ions. As beams, 6 keV N^{6+} ions and 6.15 keV O^{7+} ions were used at incidence angles of $\psi = 10°$ and $\psi = 2.5°$. As will be shown, the two incidence angles correspond to two very different classes of interac-

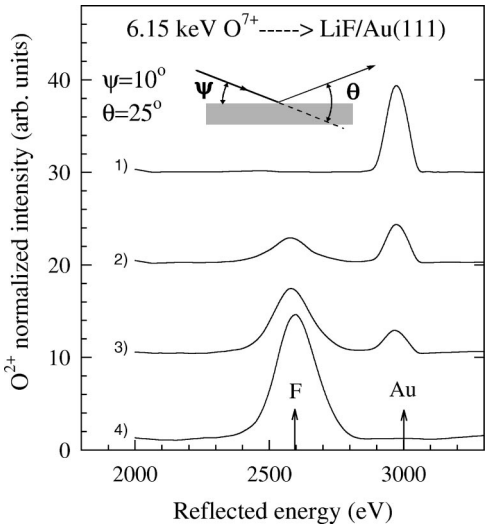

FIG. 3. Raw spectra of O^{2+} ions reflected at $\theta=25°$, from 6.15 keV O^{7+} incident at $\psi=10°$. Top spectrum is from a clean Au(111). For the three bottom spectra, the LiF coverage decreases from bottom to top. The arrows indicate the expected energy from a single elastic collision with F and Au atoms, respectively.

tions, namely for $\psi=2.5°$ the projectiles do not penetrate below the surface, while for $\psi=10°$ they do. By convention, we define the surface at the jellium edge, i.e., for Au(111) at 1.2 Å above the first atomic row [21]. The jellium edge, around which the electron density changes rapidly from bulk values to almost 0, is the place where a speeding-up of the *L*-shell filling starts [22].

The trajectories of oxygen and nitrogen ions incident along a high-indexed azimuthal direction on a Au(111) surface (20° off the ⟨100⟩ direction) were calculated by the MARLOWE code [13]. To account for the high charge state of the ions, we have calculated the image-charge acceleration according to the COB model [2]. The energy gained was added to the energy component perpendicular to the surface. In this way it is calculated that the incidence angles increase from $\psi=2.5°$ and $\psi=10°$ to $\psi=3.5°$ and $\psi=10.5°$, respectively. The MARLOWE calculations have been performed for these increased angles. This is justified since the scattering potentials are not yet effective in the region where the acceleration occurs. For 6.15 keV oxygen the trajectory results of our MARLOWE calculations are depicted in Figs. 4(a1) and 4(a2). For an incidence angle of $\psi=2.5°$ all particles scatter specularly from the Au(111) surface and their distances of closest approach to the first atomic row fall between 1.25 and 1.4 Å. For $\psi=10°$ incidence, most particles are still reflected, although a few already penetrate the target. The distances of closest approach of the reflected oxygen particles vary between 0.2 and 0.4 Å. From a point of view of interaction with target electrons, the cases of $\psi=2.5°$ and $\psi=10°$ are very different. One expects a large influence on the angular dependence of the *KLL* electron emission because of the different path lengths the electrons have to travel through the target electron density.

To get some qualitative information from the MARLOWE calculations on the influence of the LiF coverage on the scattering trajectories, LiF molecules are positioned on the surface laying along the ⟨100⟩ direction. For collisions on Au(111) covered with 1 ML of LiF, we observe a similar distinction between incidence angles of $\psi=2.5°$ and $\psi=10°$ [Figs. 4(e1) and 4(e2)] as for clean Au(111). For $\psi=2.5°$, all ions are scattered off the LiF layer, while for $\psi=10°$ most particles penetrate below the LiF layer and are scattered off the first Au layer. It is of note that a few cases are found in which the particles travel for a long distance in between the LiF and Au layer.

The results for 6 keV N^{6+} ions impinging on Au(111) and 1 ML LiF-covered Au(111) are not shown as they are similar to those of O^{7+}.

IV. *KLL* AUGER ELECTRONS FROM Au(111)

At low normal velocities, a fraction of the *KLL* Auger emission takes place above the surface. The above-surface components can be identified as sharp peaks on the low-energy side of the *KLL* spectra. The peaks exhibit a Doppler shift corresponding to emission on the incoming part of the trajectory [5–8,23]. Electrons emitted from below the surface (jellium edge) suffer attenuation and refraction [24] while crossing the electron gas and therefore exhibit an angle-dependent intensity, whereas emission above the surface will generally not depend on the emission angle. Figure 5 displays the variation of the *KLL* Auger spectra with the observation angle Θ, resulting from 6.15 keV O^{7+} ions incident at $\psi=10°$ [Fig. 5(a)] and 2.5° [Fig. 5(b)] on a clean Au(111) surface.

In all the Auger spectra, the electron energy is transformed into the projectile frame, assuming that emission occurs on the incoming trajectory, i.e., before appreciable deflection by the surface. Normalization of the spectra according to geometrical factors is hazardous and easily leads to systematic errors. To avoid such a risk, the spectra are normalized to the height of the peak at 467 eV. Typically the *KLL* spectra comprise a broad structure due to the overlapping contributions of configurations with more than two electrons in the *L* shell, and sharp peaks on the low-energy side at 467 and 482 eV, corresponding to the decay of the $1s(2s^2\ ^1S)3l^5$ and $1s(2s2p\ ^3P)3l^5$ configurations, respectively. The small peak at 512 eV is due to decay of the configuration with all captured electrons in the *L* shell, i.e., $1s2s^22p^5$, and represents the latest possible stage of the *KLL* decay.

For an incidence angle of $\psi=10°$ [Fig. 5(a)], the intensity ratio around 500 eV between the spectra measured at $\theta=50°$ and $\theta=20°$ is $I_{50}/I_{20}\approx1.3$. This part of the spectrum arises mainly from configurations with more than two *L* electrons. Those configurations are populated later in time as compared to the aforementioned configurations with two electrons in the *L* shell [$1s(2s^2\ ^1S)3l^5$ and $1s(2s2p\ ^3P)3l^5$]. Assuming that the electrons are emitted when the particles are closest to the surface (0.2–0.4 Å above the first atomic row, i.e., 0.8–1 Å below the surface) and that they are attenuated in the electron gas, we expect a ratio I_{50}/I_{20} between 1.30 and 1.45, depending on the value of the mean free path (15 and 10 Å, respectively). This is consistent with the measured ratio. It also implies that our normalization to the peak height at 467 eV is well chosen, and that the low-energy peak is essentially due to above-surface emission. It is worth noting that the small peak at 512 eV, which corresponds to configuration $1s2s^2\ 2p^5$

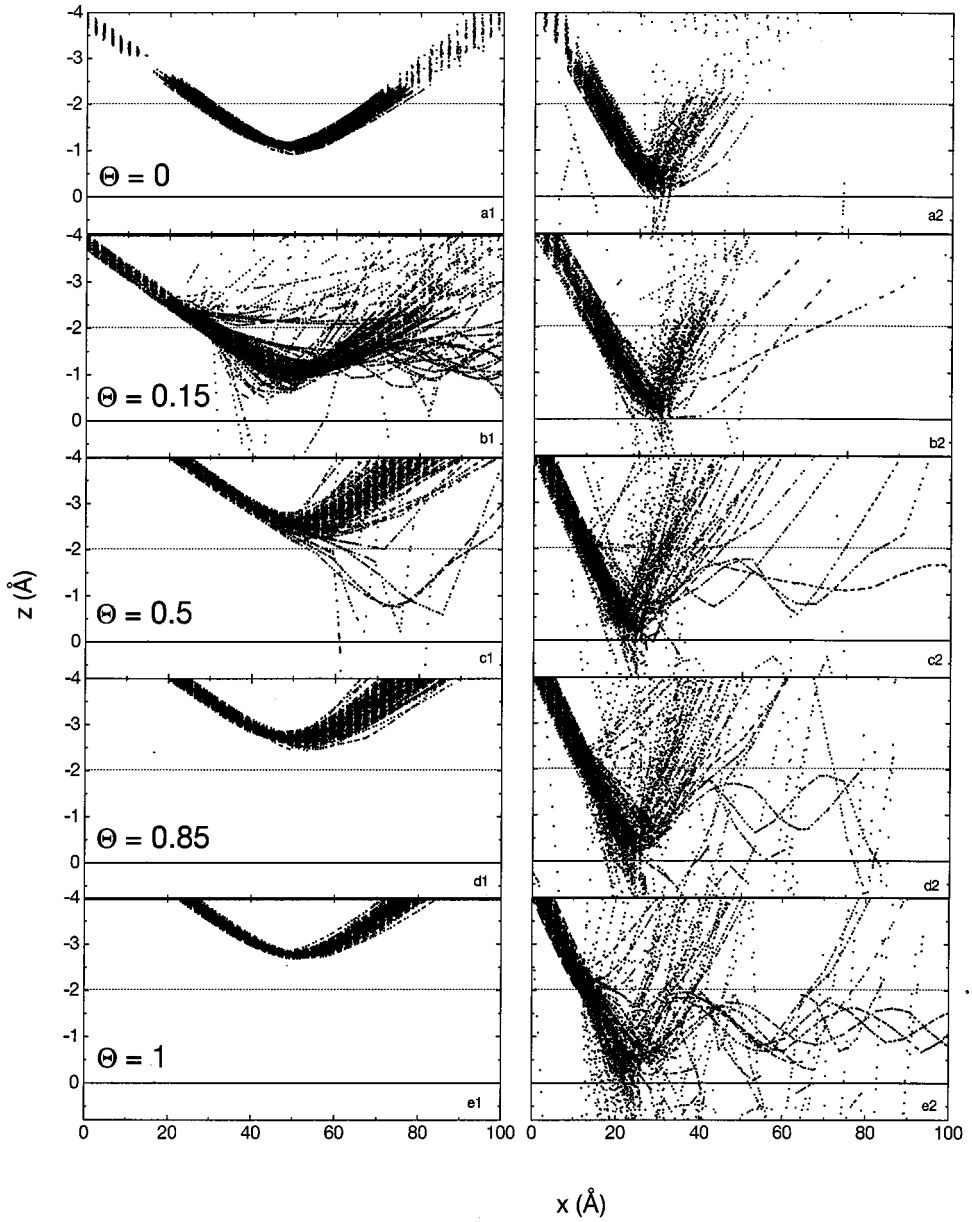

FIG. 4. MARLOWE trajectory calculations for 6 keV nitrogen projectiles incident at $\psi = 2.5°$ (left panels) and $\psi = 10°$ (right panels) on Au(111) and LiF-covered Au(111). The LiF coverage is indicated by θ. The solid lines represent the first atomic layer of Au. In panels (a1) and (a2) the dotted line represents the position of the jellium edge while in the other panels the dotted lines represent the position of the LiF layer.

(maximum number of L electrons), seems to display a Doppler shift similar to that of the low-energy peak, i.e., also being emitted on the incoming trajectory [Fig. 5(a)].

Complementary information can be drawn from the spectra obtained for $\psi = 2.5°$ [Fig. 5(b)], which show only minor changes upon variation of the observation angle. The minor angular variations indicate that the *KLL* emission occurs in regions of low electron density. This is in agreement with the trajectory calculations, which show [cf. Fig. 4(a1)] that the ions do not penetrate below the surface. Compared to $\psi = 10°$, the time between first electron capture and reaching the surface has increased from approximately 25 fs to somewhat over 100 fs. The enhanced time period above the surface explains the intensity increase of the $1s(2s^2\ ^1S)3l^5$ peak at 467 eV and the clear appearance of the $1s(2s2p\ ^3P)3l^5$ peak at 482 eV. The decay of these two configurations, which are the lowest-lying singlet and triplet ones, represents the full population of all configurations with two electrons in the L shell. The other, higher-lying states with configurations $1s(2s2p\ ^1P)3l^5$ and $1s(2p^2\ ^{1,3}L)3l^5$ decay by ultrafast Coster-Kronig transitions [26] to the lowest state within their spin system. The lifetimes of the $1s(2s^2\ ^1S)3l^5$ and the $1s(2s2p\ ^3P)3l^5$ have been calculated to be 10 and 125 fs, respectively [25,27]. Due to the Coster-Kronig channel, the higher-lying states have lifetimes of approximately 1 fs. If the complete time window from first capture to reaching the surface (100 fs) is available, the singlet system can easily fully relax and even for the triplet system about half of the population can decay. This implies that as soon as the projectiles reach the surface, the L shell is filled very fast, shifting the L-shell population from 2 to 3 to 4 . . . electrons.

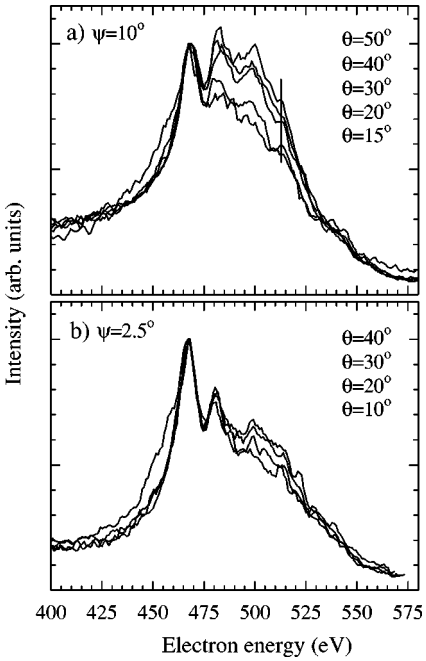

FIG. 5. Variation of *KLL* Auger emission as a function of the observation angle θ for 6.15 keV O^{7+} incident at (a) $\psi=10°$ and (b) $\psi=2.5°$. The spectra are normalized to the height of the peak at 467 eV. The electron energy is transformed into the frame of the incoming projectile, i.e., assuming that electron emission occurred on the incoming trajectory.

By solving the rate equations, Schippers *et al.* [25] calculated the relative intensities of the singlet (467 eV) and triplet (482 eV) peaks as a function of the observation time. The singlet-triplet ratio R_{ST} depends strongly on the observation period T_w. For example, when increasing T_w from 50 fs to 100 fs, R_{ST} decreases from 10 to 3. From the spectra of Fig. 5(a) one finds a ratio of about 3. Even considering the large uncertainties in the theoretical assumptions and the experimental ratio, it seems that the observation window is close to 100 fs. This implies that the time needed to get the first two electrons into the *L* shell is much shorter than 100 fs, say on the order of 10 fs.

A filling time of the order of 10 fs can also be deduced from comparing the singlet peak intensities at $\psi=10°$ and $\psi=2.5°$. At $\psi=10°$ the peak intensity is about a factor of 2 smaller. To reduce the intensity of the short-lived $1s(2s^2\ ^1S)3l^5$ configuration by a factor of 2, the observation window needs to be limited to approximately 10 fs [25]. For $\psi=10°$ the time above the surface is 25 fs, so the time to get two electrons in the *L* shell is approximately 15 fs, which is in the same range as the value estimated from the singlet-triplet ratio.

In order to study the influence of the projectile electronic structure, we performed experiments for N^{6+} ions. Figure 6 shows the angular dependence of *KLL* Auger spectra from N^{6+}-Au(111) interactions. Two differences are observed when compared to O^{7+}. First of all, the relative intensity of the singlet peak $1s(2s^2\ ^1S)3l^4$ at 352 eV is substantially lower than its equivalent from O^{7+}. This indicates that the observation-time window is much shorter than for O^{7+}. But for N^{6+} the total time between first capture and reaching the surface is only approximately 2 fs less than for O^{7+}. Such a 2-fs difference cannot explain the strong reduction in the above-surface peak. The reduction of the observation-time window is therefore likely to be caused by a reduced filling rate, i.e., an extended filling time.

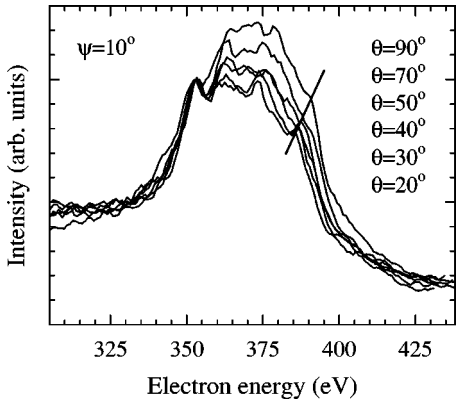

FIG. 6. Same as Fig. 5(a) but for 6 keV N^{6+}. The spectra are normalized to the height of the peak at 352 eV. The tilted line follows the position of the high-energy peak and is consistent with a Doppler shift expected for electron emission from specularly reflected projectiles.

The second difference concerns the position of the high-energy peak around 386 eV, which in contrast to O^{7+} does depend on the observation angle. The observed Doppler shift demonstrates unambiguously that it is emitted on the outgoing trajectory, i.e., following specular reflection of the projectile, as was also observed by Thomaschewski *et al.* [24]. This hints also at a reduced *L*-shell filling rate when the particles are close to the target.

Summarizing the results for a clean Au(111), we conclude that the quasimatching between the surface band structure and the projectile levels plays an important role for both the slow (above-surface) and fast (below-surface) contributions to the *L*-shell filling. Both rates are smaller for N^{6+} than for O^{7+} ions.

V. *KLL* AUGER SPECTRA FROM LiF-COVERED Au(111)

A. Experimental results

The role of the surface electronic structure in the projectile inner-shell filling is best investigated by a continuous change of the properties of the surface. Hereafter, the *KLL* Auger emission from N^{6+} and O^{7+} projectiles is monitored as a function of the LiF coverage of a Au(111) surface. We are then not only able to compare the different targets (Au, thin LiF film, and LiF bulk surface), but also we can directly observe how the changes take place. An example for the evolution of the oxygen *KLL* Auger spectrum with the LiF coverage of Au(111) is presented in Fig. 7. The 6.15 keV projectile is incident at $\psi=2.5°$ and electrons are observed at $\theta=40°$. As the LiF coverage increases, the intensity of the two low-energy peaks at 467 and 482 eV, signature of the above-surface emission, decreases. At 1 ML coverage, this above-surface component is totally suppressed and another peak appears at 457 eV, due to the decay of an incompletely screened projectile. At the higher normal velocity obtained with $\psi=10°$, a similar behavior was observed [18].

Spectra arising from the interaction of 6 keV N^{6+} on LiF-covered Au(111) are presented in Fig. 8. The beam is

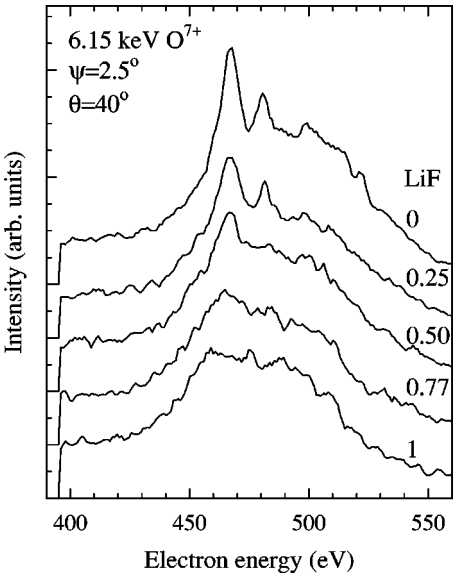

FIG. 7. *KLL* Auger spectra from LiF-covered Au(111) for varying coverage. The O^{7+} projectiles are incident at $\psi=2.5°$ and electrons are detected at $\theta=40°$. The actual coverages from 0 to 1 monolayer are indicated on the right.

incident at an angle $\psi=10°$ and electrons are observed at $\theta=30°$. In the initial stage, the evolution with LiF coverage of the intensity distribution in the Auger spectrum is quite similar to what is observed with O^{7+}: the low-energy peak from above-surface emission slowly disappears from the spectrum. Further, while approaching a monolayer, the spectrum exhibits maxima at shifted positions. We notice in particular small peaks at 342 eV and 382 eV, which correspond, respectively, to configurations $1s2s^2\,3l^3$ (singly charged projectile) and $1s2s^2\,2p^4$ (neutral projectile having a maximum number of L electrons). But most surprisingly the total *KLL* intensity increases. The intensity variation with the LiF coverage is displayed in Fig. 9, wherein the spectra are integrated over the measured energy range shown in Fig. 8. Before and after the acquisition of each spectrum, the incident

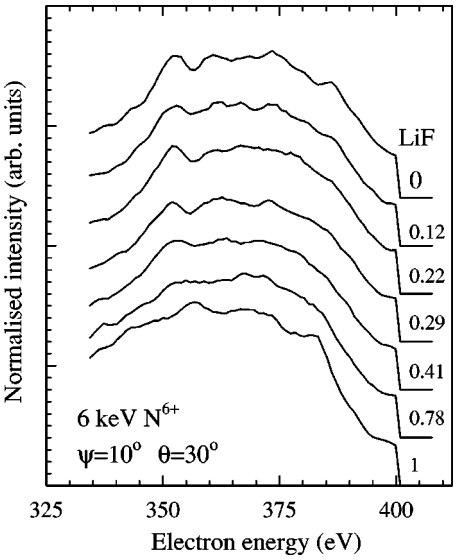

FIG. 8. Same as Fig. 7 for N^{6+} incident at $\psi=10°$; electrons are observed at $\theta=30°$. The coverage is indicated on the right.

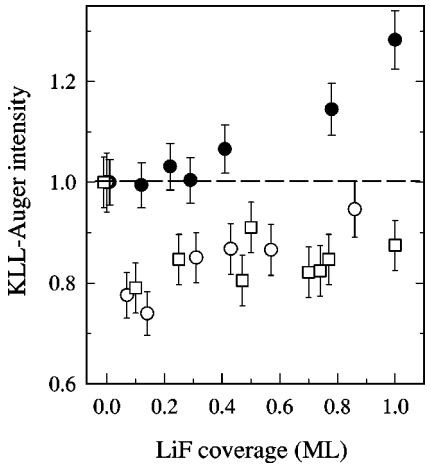

FIG. 9. Integrated *KLL* Auger intensity normalized to the intensity for clean Au as a function of LiF coverage for N^{6+} (closed symbols) projectiles incident at $\psi=10°$ and O^{7+} (open symbols) projectiles incident at $\psi=10°$ (circles) and $\psi=2.5°$ (squares).

beam current was carefully measured on a Faraday cup in front of the target, and any noticeable beam variation during acquisition could be detected on the target current recorded simultaneously. For a completed LiF overlayer, we observe an increase of nearly 30% with respect to the clean Au(111). The results for O^{7+} show a completely different behavior; after an initial decrease the total intensity recovers at 1 ML coverage to almost its initial value for clean Au.

B. Discussion

Before attempting to explain the remarkable changes in the intensities of the total *KLL* Auger spectrum as the LiF coverage increases (see Fig. 9), the spectral shapes will be discussed. To do so it is worth comparing the spectra obtained from 1 ML LiF on Au(111) not only with a clean gold target but also with results for a LiF bulk surface. Such a comparison is shown in Fig. 10 for N^{6+}. We notice the strong similarity between the LiF targets; spectra from both targets present a comparable peak structure. Furthermore, both spectra exhibit a very long tail on the low-energy side. This resemblance between 1 ML LiF and bulk LiF confirms our earlier conclusion [18] regarding the minor role played by the band gap in bulk LiF for the filling of the projectile inner shells. However, according to model calculations [3,4] the existence or absence of a band gap is relevant for the initial stages of the ion-surface interaction. This seems to imply that even the above-surface L-shell filling is not directly and fully linked to the first neutralization phase of the highly charged ion-surface interaction.

In fact, there are more aspects hinting at the existence of mechanisms that populate the L shell before the projectile penetrates into the electron gas, and which depend strongly on the system under consideration. (i) On a clean Au(111), we have seen that N^{6+} and O^{7+} behave differently, while the first neutralization steps should be similar. Namely, both above- and below-surface contributions to the *KLL* Auger spectrum are smaller for N^{6+} than for O^{7+}. (ii) For bulk LiF or 1 ML LiF/Au(111), part of the emission of *KLL* Auger electrons takes place before a complete neutralization of the projectile. This can be concluded from the extension of the

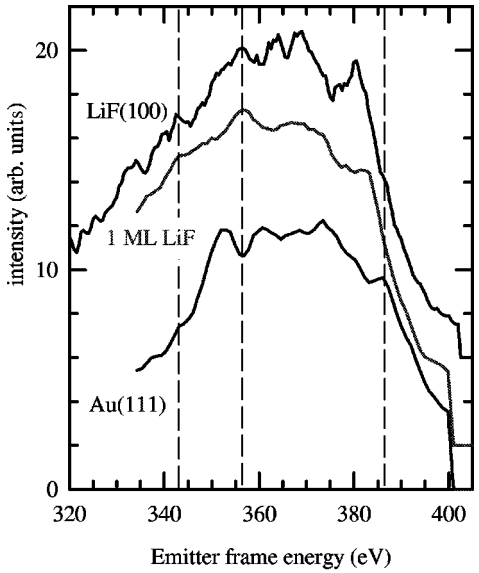

FIG. 10. Comparison of *KLL* Auger spectra from N^{6+} impinging on different targets. Top: 4 keV beam incident at $\psi=5°$ on bulk LiF(100); electrons are observed at $\theta=90°$. Middle and bottom: 6 keV beam incident at $\psi=10°$ on one-ML LiF/Au(111) and Au(111), respectively; electrons are observed at $\theta=30°$. The lines are to guide the eye.

spectrum to lower energies (see Fig. 8), indicating contributions from various ionic configurations. Such low-energy tails are not seen in the *KLL* Auger spectra from metals. For metal surfaces, *M* electrons are always available to maintain complete neutralization of the projectile above the surface, whenever Auger decay takes place. (iii) The increase of the total *KLL* Auger intensity as a function of the LiF coverage observed for N^{6+} projectiles (see Fig. 9) might be ascribed to a direct *L*-shell filling, which seems to be faster than on a clean Au surface.

This implies that other mechanisms, which depend on the system investigated, have to be invoked for explaining the observed early population of the *L* shell of the second row elements. Calculations by Arnau *et al.* [29] showed that the presence of a multiply charged ion inside a conductor induces a charge cloud made of conduction or valence electrons (*V*). This screening cloud (*C*) mimics the projectile outer shells (e.g., *M* shell for nitrogen and oxygen) and neutralizes the ion charge. The argumentation given above suggests that for metals, a similar screening cloud is already present above the surface. Thus it keeps the projectile neutral whenever autoionization transitions occur and most of all speeds up the *L*-shell filling rate [30]. To model their *KLL* spectra from N^{6+}-Au(111) interactions, Thomaschewski *et al.* [22] had to include *LCV* processes. Conduction electrons extruding into the vacuum seems natural in view of the high fields involved. Bardsley and Penetrante [31] have shown, using a classical dynamics model of the highly charged ion-surface interaction, that indeed many unbound electrons are present around the ion well above the surface, and that they effectively screen the ion charge. Additionally they calculated that electrons extracted from the solid when the projectile is closer to the surface populate deeply bound orbitals [32].

The quasiresonant filling process is also a valid candidate for explaining the observed early transfer of electrons to inner shells. For instance, such a filling of the oxygen *L* shell from Au valence electrons was shown to be a very efficient way for achieving fast neutralization and relaxation of O^{7+} between the jellium edge and the first atomic layer [2]. The direct filling of projectile inner shells from the valence electrons at large distance was also inferred from the interaction of Ar^{17+} with a graphite surface [33]. To reproduce the observed x-ray spectrum and its dependence on the impact angle, the authors used a simple neutralization model that assumes a single *M*-shell filling process above and below the surface. The model describes rather well the early *M*-shell population.

Additionally, in particular above nonmetallic surfaces when resonant neutralization is less efficient, Auger neutralization and deexcitation processes may play a role. Direct *L*-shell filling from capture of target core electrons is also a possibility [34,35]. Direct capture from target inner shells requires close encounters, which are not achieved in most collisions where a fast neutralization and relaxation of the multiply charged ion is observed (see, e.g., [36]).

The gain of intensity in the nitrogen *KLL* Auger spectrum as the LiF coverage increases (see Fig. 9) is remarkable and represents a new aspect in the neutralization of highly charged ions above surfaces. At first sight, this indicates a more efficient nitrogen *L*-shell filling from LiF than from Au, which is consistent with the conclusion drawn from Fig. 6 that the nitrogen *L*-shell filling from a clean Au(111) is particularly slow.

According to MARLOWE calculations of trajectories on the clean Au(111) surface [Fig. 4(a2)], 95% of the projectiles are reflected above the first layer, at a depth less than 1.2 Å below the jellium edge. Assuming that most of the electrons are emitted at that position and taking a mean free path of 10 Å [28], this would lead to an attenuation around 30%. Therefore, the intensity gain measured on a monolayer LiF seems to cancel the intensity attenuation experienced in the clean Au(111) target. But as Fig. 4(e2) shows, only a small fraction of the ions is reflected off the LiF layer; the majority of the trajectories penetrates below the LiF and enters the electron gas of the Au. It is therefore unlikely that trajectory effects alone can explain the increase, in particular since the trajectories for N^{6+} and O^{7+} are similar. The behavior of the O^{7+} results is more in line with what one would expect from the MARLOWE calculations. For example, if one looks at the left panels of Fig. 4, one sees that at small coverages (4b1) some of the trajectories come closer to the first atomic layer of the Au(111) surface, and a few even penetrate. A loss of intensity is thus expected. When the coverages approach a full monolayer [cf. Figs. 4(d1) and 4(e1)] all particles are reflected from the LiF layer, thereby diminishing the distance emitted electrons have to travel through the electron gas. An initial decrease in intensity followed by an increase at higher coverages is indeed observed in the measurements (cf. Fig. 9). The intensity increase for N^{6+} is therefore most likely due to a more efficient filling of the *L* shell on LiF as com-

pared to Au. An indication of efficient *L*-shell filling for the N^{6+}-LiF system is also found from the work of Limburg *et al.* [12] at higher energies on bulk LiF. They observed strong peaks in their *KLL* spectra corresponding to the maximum *L*-shell filling for N^{6+}, while for O^{7+} these peaks were only just visible. The large differences observed between the two species can only be understood on the grounds of their different electronic structures. Hence, we conclude that for 1 ML LiF on Au(111), most nitrogen *KLL* Auger electrons are emitted above the LiF overlayer.

VI. CONCLUSION

In summary, we have used thin LiF films on Au(111) to study the neutralization dynamics of N^{6+} and O^{7+} projectiles at grazing incidence. The use of different projectile species, together with the possibility to change the nature of the surface during a single experimental run, allows us to draw definite conclusions regarding the inner-shell filling above the first atomic layer.

(i) For a clean Au(111) surface, the *L*-shell filling is faster for O^{7+} than for N^{6+}. This can be concluded from the comparison of oxygen and nitrogen *KLL* Auger spectra obtained for similar conditions, and it is visibly independent of whether the electron emission occurrs before or after the projectile reaches the bulk electron density.

(ii) As opposed to this, for a LiF-covered Au(111) surface the *L*-shell filling is faster for N^{6+} than for O^{7+}. Especially remarkable in this connection is the increase of the intergrated N^{6+} total Auger intensity with increasing LiF coverage of the Au(111) surface, whereby the gain is mainly due to emission from a doubly filled *L* shell. However, for both N^{6+} and O^{7+} the projectile neutralization is not always completed at the moment of electron emission.

(iii) The band gap in LiF plays only a minor role for the hollow atom dynamics. This confirms our earlier conclusion [18] and is based on the similarity of spectra obtained with bulk LiF targets and LiF-covered Au(111) targets, respectively.

(iv) The *L*-shell filling mechanisms just above and below the jellium edge seem to be the same: there is no indication for different processes in these two regions. Apparently there is a continuous evolution from the first step of neutralization to the capture into inner shells.

(v) Finally it can be concluded that ''above-surface'' electron emission is not necessarily leading to sharp peaks in the spectra. Especially for the LiF targets, a broadened electron distribution with a low-energy tail results from Auger decay of several, overlapping ionic configurations.

The dynamics of the hollow atom/ion above the surface represents certainly the most critical part of the interaction between a highly charged ion and a surface. We believe that many subtle aspects are yet to be unraveled. For that respect, thin films represent a versatile tool for studying *in situ* the target dependence of the mechanisms involved in the inner-shell neutralization and relaxation. This allows changing well defined surface quantities while keeping all other experimental conditions constant. Further experiments are underway for determining the influence of the various solid-state properties (e.g., the valence electron density and the width of the valence band) in the hollow atom/ion dynamics at the surface.

ACKNOWLEDGMENTS

This work is part of the research program of the Stichting voor Fundamenteel Onderzoek der Materie (FOM) with financial support from the Nederlandse Organisatie voor Wetenschappelijk Onderzoek (NWO). One of us (T.S.) was supported by the EU TMR program under Grant No. ERBFMBICT961704.

[1] A. Arnau *et al.*, Surf. Sci. Rep. **27**, 117 (1997), and references therein.
[2] J. Burgdörfer, P. Lerner, and F.W. Meyer, Phys. Rev. A **44**, 5674 (1991).
[3] L. Hägg, C.O. Reinhold, and J. Burgdörfer, Phys. Rev. A **55**, 2097 (1997).
[4] J.J. Ducrée, F. Casali, and U. Thumm, Phys. Rev. A **57**, 338 (1998).
[5] F.W. Meyer, S.H. Overbury, C.C. Havener, P.A. Zeijlmans van Emmichoven, and D.M. Zehner, Phys. Rev. Lett. **67**, 723 (1991).
[6] H.J. Andrä, A. Simionovici, T. Lamy, A. Brenac, and A. Pesnelle, Europhys. Lett. **23**, 361 (1993).
[7] M. Grether, A. Spieler, R. Köhrbrück, and N. Stolterfoht, Phys. Rev. A **52**, 426 (1995).
[8] J. Limburg, S. Schippers, I. Hughes, R. Hoekstra, R. Morgenstern, S. Hustedt, N. Hatke, and W. Heiland, Phys. Rev. A **51**, 3873 (1995).
[9] J.P. Briand, S. Thuriez, G. Giardino, G. Borsoni, M. Froment, M. Eddrief, and C. Sébenne, Phys. Rev. Lett. **77**, 1452 (1996).
[10] J. Limburg, S. Schippers, R. Hoekstra, R. Morgenstern, H. Kurz, F. Aumayr, and H.P. Winter, Phys. Rev. Lett. **75**, 217 (1995).
[11] S. Pülm, A. Hitzke, J. Günster, H. Müller, and V. Kempter, Radiat. Eff. Defects Solids **128**, 151 (1994).
[12] J. Limburg, S. Schippers, R. Hoekstra, R. Morgenstern, H. Kurz, M. Vana, F. Aumayr, and H.P. Winter, Nucl. Instrum. Methods Phys. Res. B **115**, 237 (1996).
[13] M.T. Robinson and I.M. Torrens, Phys. Rev. B **9**, 5008 (1974).
[14] H. Niehus, W. Heiland, and E. Taglauer, Surf. Sci. Rep. **17**, 213 (1993).
[15] H.H. Brongersma and J.P. Jacobs, Surf. Sci. **75**, 133 (1994).
[16] U. Diebold, J.M. Pan, and T.E. Madey, Surf. Sci. **331-333**, 845 (1995).
[17] T. Neidhart, Z. Toth, M. Hochhold, M. Schmid, and P. Varga, Nucl. Instrum. Methods Phys. Res. B **90**, 496 (1994).
[18] H. Khemliche, T. Schlathölter, R. Hoekstra, R. Morgenstern, and S. Schippers, Phys. Rev. Lett. **81**, 1219 (1998).
[19] T. Hecht, C. Auth, A.G. Borisov, and H. Winter, Phys. Lett. A **220**, 102 (1996).

[20] T. Neidhart, F. Pichler, F. Aumayr, H.P. Winter, M. Schmid, and P. Varga, Phys. Rev. Lett. **74**, 5280 (1995).
[21] A. Zangwill, *Physics at Surfaces* (Cambridge University Press, Cambridge, UK, 1988).
[22] J. Thomaschewski, J. Bleck-Neuhaus, M. Grether, A. Spieler, and N. Stolterfoht, Phys. Rev. A **57**, 3665 (1998).
[23] F.W. Meyer, S.H. Overbury, C.C. Havener, P.A. Zeijlmans van Emmichoven, J. Burgdörfer, and D.M. Zehner, Phys. Rev. A **44**, 7214 (1991).
[24] J. Thomaschewski, J. Bleck-Neuhaus, M. Grether, A. Spieler, D. Niemann, and N. Stolterfoht, Nucl. Instrum. Methods Phys. Res. B **125**, 163 (1997).
[25] S. Schippers, J. Limburg, J. Das, R. Hoekstra, and R. Morgenstern, Phys. Rev. A **50**, 540 (1994); **50**, 4229 (E) (1994).
[26] J. Limburg, J. Das, S. Schippers, R. Hoekstra, and R. Morgenstern, Phys. Rev. Lett. **73**, 786 (1994).
[27] J.E. Hansen, O. Schraa, and N. Vaeck, Phys. Scr. **T41**, 41 (1992).
[28] G. A. Somorjai, *Chemistry in Two Dimensions: Surfaces* (Cornell University Press, Ithaca, NY, 1981).
[29] A. Arnau, P.A. Zeijlmans van Emmichoven, J.I. Juaristi, and E. Zaremba, Nucl. Instrum. Methods Phys. Res. B **100**, 279 (1995).
[30] N. Vaeck and J.E. Hansen, Surf. Sci. **270**, 596 (1992).
[31] J.N. Bardsley and B.M. Penetrante, Comments At. Mol. Phys. **27**, 43 (1991).
[32] J. Burgdörfer, C. Reinhold, and F.W. Meyer, Nucl. Instrum. Methods Phys. Res. B **98**, 415 (1995).
[33] S. Winecki, C.L. Cocke, D. Fry, and M.P. Stöckli, Phys. Rev. A **53**, 4228 (1996).
[34] F.W. Meyer, C.C. Havener, S.H. Overbury, K.J. Reed, K.J. Snowdon, and D.M. Zehner, J. Phys. (Paris), Colloq. **50**, C1-263 (1989).
[35] M. Grether, D. Niemann, A. Spieler, and N. Stolterfoht, Phys. Rev. A **56**, 3794 (1997).
[36] L. Folkerts, S. Schippers, D.M. Zehner, and F.W. Meyer, Phys. Rev. Lett. **74**, 2204 (1995).